ARTICULATED AND DEFORMABLE MOTION ANALYSIS FROM MOTION CAPTURE DATA

J. K. Fayad*, A. Del Bue# e P. M. Q. Aguiar+

*- *QueenMary, University of London; jrkf@dcs.qmul.ac.uk*

#- *Instituto de Sistemas e Robótica – Instituto Superior Técnico; adb@isr.ist.ult.pt*

+- *Instituto de Sistemas e Robótica – Instituto Superior Técnico; aguiar@isr.ist.utl..pt*

KEY WORDS: Gait analysis, Human body models, Factorization, Non-linear modelling, Biomechanics.

ABSTRACT: *Human 3D models and motion analysis are nowadays used in a wide range of applications, spanning from medicine to security and surveillance. In this work, we will focus on the creation of biomechanical models for clinical and sports analysis.*

Nowadays, motion capture systems accurately measure the 3D coordinates of reflective markers place above the skin. Here we present a general framework to automatically recover joint parameters modelling the human articulations from the 3D coordinates of a point cloud provided by motion capture systems. Additionally, we describe an approach capable of recovering a more accurate rigid body description of non-rigid bodies. We then propose a new quadratic model to explain soft-tissue artefacts formed as a natural extension of the existing rigid body models. Finally we use synthetic data to assess the performance of the algorithms and to compare the results with ground truth data. Qualitative analyses of real data sequences over different motion capture databases are also presented.

1 INTRODUCTION

Computational models of human articulations are fundamental to perform an accurate analysis of the mechanical motion of a human body. Applications of these models span various fields, ranging from engineering to life sciences, where the analysis of human motion is crucial to perform accurate clinical analysis and credible animations of skeleton models [1]. In this work we will focus on the task of building biomechanical models of the human body from motion capture (MOCAP) systems.

MOCAP systems are devices able to recover a 3D description of the motion of a shape (see [2] for a complete review of the state of the art). The output of these systems is the 3D coordinates of feature points over time.

One of the main problems of existing methods for joint parameter estimation based on MOCAP systems is their *limited repeatability* [1]. This is a strong setback on their applications as accuracy and repeatability is of extreme importance in clinical analysis. Another major source of error in these analyses are *soft-tissue artefacts* [3, 4, 5]. The relevant information about articulations used to build human models is given by the skeleton. At this scale, bones can be considered to be rigid. However, the markers tracked by MOCAP systems are placed above the skin. As there is an inherent relative motion between the soft-tissues surrounding bone and bone itself, data artefacts arise and performance is degraded.

A key step in joint parameter estimation is the *model calibration* [1]. To obtain clinically relevant data, the model must be subject specific. Most of current methods use some sort of regression technique to fit the models to the subjects, limiting the method to the quality of the regression. On the other hand, a great number of these methods require markers to be placed at specific anatomical landmarks. Such positioning is affected by human errors and it has the further problem of not always being possible to locate those landmarks. Thus, methods that do not rely on specific landmarks locations would be preferred.

In this work we propose methods to semi-automatically compute human skeleton models while dealing with the current limitations of the existent methods. Using recent developments in Structure from Motion (SfM) algorithms that allow retrieval of articulated structures from a set of 2D images [6, 7], we propose a method to extract joint parameters based on the 3D coordinates provided by the MOCAP systems. This approach does not depend on the process by which the data was acquired. The single assumption here is the initial assignment of each 3D point to the respective body segment. Inspired by previous works on the field of computer graphics [8, 9] we present a new quadratic model for non-rigid bodies. This model expands the existing linear model for rigid bodies by including quadratic terms, which allows us to model non-rigid bodies. By modelling non-rigid bodies we will be able to separate the rigid contribution (skeleton) from the non-rigid one (soft-tissue) and provide more accurate estimates for the joint models.

2 RIGID BODY FACTORIZATION

Factorization methods for SfM are a family of image based algorithms that model moving objects as a product of two factors: *motion* and *shape*. Our factorization approach assumes a set of *P* 3D points being tracked over *F* frames by a MOCAP system. This method relies on the key fact that 3D trajectories of points belonging to the same body share the same global properties. Thus, we can define a motion matrix **W** containing the 3D coordinates of *P* points over *F* frames as:

$$\mathrm{W} = \begin{bmatrix} \mathrm{W}_1 \\ \mathrm{W}_2 \\ \vdots \\ \mathrm{W}_F \end{bmatrix} = \begin{bmatrix} \mathrm{R}_1 \\ \mathrm{R}_2 \\ \vdots \\ \mathrm{R}_F \end{bmatrix} \begin{bmatrix} x_1 x_2 \cdots x_P \\ y_1 y_2 \cdots y_P \\ z_1 z_2 \cdots z_P \end{bmatrix} + \begin{bmatrix} \mathrm{T}_1 \\ \mathrm{T}_2 \\ \vdots \\ \mathrm{T}_F \end{bmatrix} = \mathrm{MS+T}, \quad (1)$$

where $\mathbf{R}_i$ is a 3 × 3 rotation matrix, $\mathbf{T}_i$ is a 3 × P matrix representing the translation and **S** is a 3 × P matrix containing the local coordinates of the P points. The translational component can be computed as the coordinates of the centroid of the point cloud at each frame $\mathbf{W}_i$. Thus it can be easily eliminated by registering, at each frame, the point cloud to the origin. In this scenario it frequently occurs that instead of **W** we consider a registered version $\hat{\mathbf{W}}$ defined as:

$$\hat{\mathrm{W}} = \mathrm{W} - \mathrm{T} = \mathrm{M}\,\mathrm{S} \quad (2)$$

2.1 INDEPENDENT BODY MOTION

Considering the model defined in eq. (1) for a single body, it follows that $rank(\mathbf{W}) \leq 4$ [10]. On the other hand if we defined the system without the translational component as in eq. (2) we have that $rank(\hat{\mathbf{W}}) \leq 3$. However, when performing real experiments, there will always be noise involved which will increase the rank of $\hat{\mathbf{W}}$.

Let us consider the rank-3 truncated SVD $\mathbf{W} = \mathbf{U}_3\ \mathbf{\Sigma}_3\ \mathbf{V_3}^{\mathrm{T}}$. This decomposition is not only useful for noise reduction, as we apply an ideal rank constraint to the data matrix, but it can also be used as the starting point for the factorization algorithm. Considering the expected dimensions of **M** and **S,** we can compute a first estimation as $\hat{\mathrm{M}} = \mathrm{U}_3\Sigma_3^{1/2}$ and $\mathrm{S} = \Sigma_3^{1/2}\mathrm{V}_3^{T}$. However there exists an ambiguity in this factorization as $\mathrm{W} = \hat{\mathrm{M}}\,\mathrm{Q}\,\mathrm{Q}^{-1}\hat{\mathrm{S}} = \mathrm{M}\,\mathrm{S}$. Since this factorization does not guarantee that $\hat{\mathrm{M}}$ is in fact a collection of *F* rotation matrices, the

ambiguity is solved by finding the matrix **Q** that will transform each 3×3 matrix $\hat{M}_i$ in a rotation matrix $\mathbf{R}_i$. This can be achieved by imposing the orthogonality of $\mathbf{R}_i$ (see [10] for details).

2.2 UNIVERSAL JOINT

By universal joint, we mean a joint in which each of the two bodies is at a fixed distance to the joint centre. In this scenario, the relative position of the bodies is constrained but their rotations remain independent. A scheme of this joint is presented in Fig. 1.

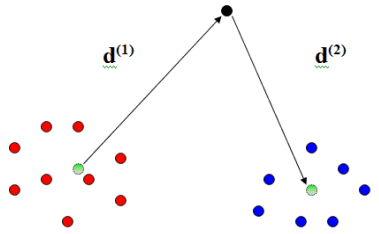

Fig. 1 Scheme of a universal joint. The 3-vectors $\mathbf{d}^{(1)}$ and $-\mathbf{d}^{(2)}$ are respectively the 3D coordinates of the joint centre in the local referential of the first and second body.

Let $\mathbf{d}^{(1)} = [u, v, w]^T$ be the 3D coordinates of the joint centre in the local referential of the first body; $-\mathbf{d}^{(2)} = [u', v', w']^T$ be the 3D coordinates of the joint centre in the local referential of the second body; $\mathbf{R}^{(1)}$ and $\mathbf{R}^{(2)}$ the $3F \times 3$ matrices corresponding to a collection of F 3×3 global rotation matrices; $\mathbf{t}^{(1)}$ and $\mathbf{t}^{(2)}$ the $3F$-vectors corresponding to the translation vectors.

The joint centre can thus be seen as a point that belongs to both bodies and so its position can be described using the motion equations for the first and second body. With these considerations, a geometrical analysis of the joint reveals that:

$$\mathrm{R}^{(1)}\mathrm{d}^{(1)} + \mathrm{t}^{(1)} = -\mathrm{R}^{(2)}\mathrm{d}^{(2)} + \mathrm{t}^{(2)}. \qquad (3)$$

Thus we can state that both 4D subspaces have a 1D intersection. The result of this consideration is that $rank(\mathbf{W}) \leq 7$, one dimension less when comparing to the case of two independent where $rank(\mathbf{W}) \leq 8$. We are now able to factorize the measurement matrix as:

$$\mathrm{W} = \begin{bmatrix} \mathrm{W}^{(1)} & \mathrm{W}^{(2)} \end{bmatrix} = \begin{bmatrix} \mathrm{R}^{(1)}\mathrm{R}^{(2)}\mathrm{t}^{(1)} \end{bmatrix} \begin{bmatrix} \mathrm{S}^{(1)} & \mathrm{D}^{(2)} \\ & \mathrm{S}^{(2)} + \mathrm{D}^{(2)} \\ 1_{P_1}^{\mathrm{T}} & 1_{P_2}^{\mathrm{T}} \end{bmatrix}, \qquad (4)$$

where $\mathbf{W}^{(1)}$ and $\mathbf{W}^{(2)}$ are respectively the measurement matrices for the first and second body; $\mathbf{D}^{(2)} = \mathbf{d}^{(2)}.\ \mathbf{1}_{P2}{}^{\mathrm{T}}$, with $\mathbf{1}_{P2}$ is a P_2-vector with all entries equal to 1, where P_2 is the number of points belonging to the second body. The same applies for $\mathbf{1}_{P1}{}^{\mathrm{T}}$. Notice that in order to separate $\mathbf{W}^{(1)}$ from $\mathbf{W}^{(2)}$, we must assume the body segmentation to be known.

To recover the structure of the joint one needs to find $\mathbf{d}^{(1)}$ and $\mathbf{d}^{(2)}$. From eq. (3) we can write:

$$\begin{bmatrix} \mathrm{R}^{(1)} & \mathrm{R}^{(2)} & \mathrm{t}^{(2)} - \mathrm{t}^{(1)} \end{bmatrix} \begin{bmatrix} \mathrm{d}^{(1)} \\ \mathrm{d}^{(2)} \\ -1 \end{bmatrix} = 0, \qquad (5)$$

where $\mathbf{S}^{(1)}$ is a $3 \times P_1$ global shape matrix for the first body and $\mathbf{S}^{(2)}$ is a $3 \times P_2$ global shape matrix for the second body. The initial step in the factorization is again done by performing an SVD and by keeping the first six components:

$$\tilde{\mathrm{W}} = \mathrm{U}_6 \Sigma_6^{1/2} \Sigma_6^{1/2} \mathrm{V}_6^T = \begin{bmatrix} \mathrm{U}^{(1)} & \mathrm{U}^{(2)} \end{bmatrix} \begin{bmatrix} \mathrm{V}^{(1)} & \mathrm{V}^{(2)} \end{bmatrix}. \qquad (6)$$

However $[\mathbf{V}^{(1)} \mid \mathbf{V}^{(2)}]$ is a dense matrix while the registered structure matrix block diagonal. If we define an operator $N_l(.)$ that returns the left null-space of its argument, we can define a 6×6 transformation matrix $\mathbf{T}_U$ such that we can recover **S** by pre-multiplying it with $\mathbf{T}_U$:

$$\mathrm{T}_U\ \mathrm{S} = \begin{bmatrix} N_l(\mathrm{V}^{(2)}) \\ N_l(\mathrm{V}^{(1)}) \end{bmatrix} \begin{bmatrix} V(1) & V(2) \end{bmatrix} = \begin{bmatrix} \mathrm{S}^{(1)} & 0 \\ 0 & \mathrm{S}^{(2)} \end{bmatrix}. \qquad (7)$$

To keep the original data unaltered, we do $[\mathbf{M}^{(1)}\ \mathbf{M}^{(2)}] = \mathbf{T}_U{}^{-1}\ [\mathbf{U}^{(1)} \mid \mathbf{U}^{(2)}]$. Note that the ambiguity seen in Section 2.1 is still present for each body, being no guarantee that $\mathbf{M}^{(1)}$ or $\mathbf{M}^{(2)}$ are a collection of 3×3 rotation matrices. Due to the specific configuration of **S** seen in

eq. (9), there is no linear method to impose the orthogonality constraints to **M** while assuring that structure for **S**. We thus treat each body separately as done in Section 2.1.

2.3 HINGE JOINT

In a hinge joint, two bodies can rotate around an axis such that the distance to that rotation axis is constant. Therefore their rotation matrices $\mathbf{R}^{(1)}$ and $\mathbf{R}^{(2)}$ are not completely independent. A scheme of the hinge joint is presented in Fig. 2.

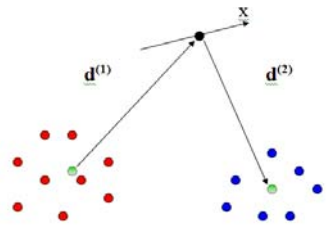

Fig. 2 Scheme of a hinge joint. The 3-vectors $\mathbf{d}^{(1)}$ and $-\mathbf{d}^{(2)}$ are respectively the 3D coordinates of the joint centre in the local referential of the first and second body. The hinge axis is represented by the x-axis.

In this kind of joint, any vector belonging to any of the two bodies that is parallel to the joint axis must remain so throughout the movement. Let us choose an appropriate local referential, without loss of generality, where the axis of rotation of the joint is coincident with the x-axis. To comply with the hinge joint constraint, the first column of $\mathbf{R}^{(1)}$ must be equal to the first column of $\mathbf{R}^{(2)}$. Thus, we define the rotation matrices as $\mathbf{R}^{(1)} = [\mathbf{c}_1\ \mathbf{c}_2\ \mathbf{c}_3]$ and $\mathbf{R}^{(2)} = [\mathbf{c}_1\ \mathbf{c}_4\ \mathbf{c}_5]$.

All the points belonging to the rotation axis must fulfil both movement conditions. Thus, there is a 2D intersection of the original 4D subspaces. Since the joint constraint applies only on the rotation factor, we will consider the registered form of the problem. This will result in a rank-5 matrix $\hat{\mathbf{W}}$ defined by:

$$\tilde{\mathrm{W}} = \begin{bmatrix} \mathrm{c}_1 & \mathrm{c}_2 & \mathrm{c}_3 & \mathrm{c}_4 & \mathrm{c}_5 \end{bmatrix} \begin{bmatrix} x_1^{(1)} \cdots x_{P_1}^{(1)} & x_1^{(2)} \cdots x_{P_2}^{(2)} \\ y_1^{(1)} \cdots y_{P_1}^{(1)} & 0 \ \cdots \ 0 \\ z_1^{(1)} \cdots z_{P_1}^{(1)} & 0 \ \cdots \ 0 \\ 0 \ \cdots \ 0 & y_1^{(2)} \cdots y_{P_2}^{(2)} \\ 0 \ \cdots \ 0 & z_1^{(2)} \cdots z_{P_2}^{(2)} \end{bmatrix}, \quad (8)$$

Once again we use the truncated SVD of $\hat{\mathbf{W}}$ as the first step on the parameter estimation. The process is the same as the one used in Section 2.2 for the hinge joint, except now $[\mathbf{U}^{(1)}|\mathbf{U}^{(2)}]$ is a $3F \times 5$ matrix, and $[\mathbf{V}^{(1)} \mid \mathrm{V}^{(2)}]$ is a $5 \times (P_1 + P_2)$ matrix. As the first row of S is dense, we define $\mathbf{T}_\mathrm{H}$ as a transformation matrix such that:

$$\mathrm{T}_H = \begin{bmatrix} \mathrm{b}^T \\ Nl(\mathrm{V}^{(2)}) \\ Nl(\mathrm{V}^{(1)}) \end{bmatrix}, \quad (9)$$

where $\mathbf{b}^\mathrm{T} = [1\ 0\ 0\ 0\ 0\ 0]$. By pre-multiplying $[\mathbf{V}^{(1)} \mid \mathbf{V}^{(2)}]$ with $\mathbf{T}_\mathrm{H}$ we leave the first row intact and we zero-out some entries in order to get the structure presented in eq. (8). As seen before, we also post-multiply $[\mathbf{U}^{(1)}|\mathbf{U}^{(2)}]$ with $\mathbf{T}_\mathrm{H}$. Again we must impose orthogonality constraints on the recovered motion matrices in order to solve the ambiguity. This is done in the same way as in Section 2.2 for the universal joint. In this case, the joint centre can lie anywhere on the axis of rotation. Still it must obey the motion equations for both bodies. Combining eq. (5) with the properties of $\mathbf{R}^{(1)}$ and $\mathbf{R}^{(2)}$ for the hinge joint, the joint parameters can now be estimated by:

$$\begin{bmatrix} \mathrm{c}_1 & \mathrm{c}_2 & \mathrm{c}_3 & \mathrm{c}_4 & \mathrm{c}_5 & \mathrm{t}^{(2)} - \mathrm{t}^{(1)} \end{bmatrix} \begin{bmatrix} u + u' \\ v \\ w \\ v' \\ w' \\ -1 \end{bmatrix} = 0\,. \quad (10)$$

3 WEIGHTED FACTORIZATION

When dealing with non-rigid objects, factorizing with the previous algorithms can be seen as averaging the shape throughout the frames, resulting in an attenuation of the deformations. Inspired by [11], we present an approach that uses a weighted SVD in order to penalise the contribution of the points which deform most. By doing so we will attenuate the deformations contribution and we will attain a more accurate rigid representation of the body. Let us consider a rearrangement of the data matrix as:

$$\mathrm{W} = \begin{bmatrix} {w_{11}}^T & \cdots & {w_{1P}}^T \\ \vdots & \ddots & \vdots \\ {w_{F1}}^T & \cdots & {w_{FP}}^T \end{bmatrix}, \qquad (11)$$

which is now an $F \times 3P$ matrix. Let us also define $\hat{\mathbf{W}}^{(\mathbf{r})}$ as the best rigid description of a given non-rigid body. The distance between the best rigid description of a point j and the position estimated by the rigid body factorization can be given by $||\mathrm{E_j}|| = ||\hat{\mathbf{W}}_\mathbf{j}^{(\mathbf{r})} - \hat{\mathbf{W}}_\mathbf{j}||$. The deviation from the best description can be seen as a measure of the non-rigidity of the point. Thus a weighted factorization method can be created as a minimization of the following cost function:

$$\arg\min_{\mathrm{M_i},s_j} \sum_{i=1}^{F}\sum_{j=1}^{P} (\tilde{w}_{ij}^{(r)} - \mathrm{M_i s_j})^T \mathrm{C_j} (\tilde{w}_{ij}^{(r)} - \mathrm{M_i s_j}) \qquad (13)$$

where $\mathbf{C}_\mathrm{j} = \mathrm{cov}(\mathbf{E}_\mathrm{j})^{-1}$ is the weight matrix. However we do not know the best rigid description of a body, nor do we know the weight matrix. Thus we created a double step iterative algorithm that computes the motion and shape parameters in one step, the weight matrix on the other (for more details, see [12]). This algorithm is initialized by the result of the rigid body factorization.

4 QUADRATIC MODEL FORMULATION

Our model expands the rigid body formulation defined by eq. (1), to a formulation that uses linear, quadratic and crossed-terms of the previous rigid shape matrix, while keeping the same factorization-based approach. Let us define the new shape matrix as in eq. (14), where $\mathbf{S}^{(\mathbf{\Gamma})}$ is the $3 \times P$ linear shape matrix, $\mathbf{S}^{(\mathbf{\Omega})}$ the $3 \times P$ quadratic shape matrix and $\mathbf{S}^{(\Lambda)}$ is the $3 \times P$ cross-values shape matrix. Given this new structure of $\mathbf{S}$, the data matrix can be defined as in eq. (15), where where $\mathbf{R}_\mathrm{i}$ is a 3×3 rotation matrix, and $\mathbf{\Gamma}_\mathrm{i}$ is a 3×3 transformation matrix associated with linear deformations, $\mathbf{\Omega}_\mathrm{i}$ is a 3×3 transformation matrix associated with quadratic transformations and $\mathbf{\Lambda}_\mathrm{i}$ is a 3×3 transformation associated with cross-values deformations.

$$\mathrm{S} = \begin{bmatrix} x_1 & \cdots & x_P \\ y_1 & \cdots & y_P \\ z_1 & \cdots & z_P \\ {x_1}^2 & \cdots & {x_P}^2 \\ {y_1}^2 & \cdots & {y_P}^2 \\ {z_1}^2 & \cdots & {z_P}^2 \\ x_1y_1 & \cdots & x_Py_P \\ y_1z_1 & \cdots & y_Pz_P \\ z_1x_1 & \cdots & z_Px_P \end{bmatrix} = \begin{bmatrix} \mathrm{S}^{(\Gamma)} \\ \mathrm{S}^{(\Omega)} \\ \mathrm{S}^{(\Lambda)} \end{bmatrix}, \qquad (14)$$

$$\tilde{\mathrm{W}} = \begin{bmatrix} \mathrm{R}_1 & & & \\ & \mathrm{R}_2 & & \\ & & \ddots & \\ & & & \mathrm{R}_\mathrm{F} \end{bmatrix} \begin{bmatrix} \Gamma_1 & \Omega_1 & \Lambda_1 \\ \Gamma_2 & \Omega_2 & \Lambda_2 \\ & \cdots & \\ \Gamma_P & \Omega_P & \Lambda_P \end{bmatrix} \begin{bmatrix} \mathrm{S}^{(\Gamma)} \\ \mathrm{S}^{(\Omega)} \\ \mathrm{S}^{(\Lambda)} \end{bmatrix}. \qquad (15)$$

Note that the deformations are defined in the local referential of the body. In this case the model is described by a *rank*($\hat{\mathbf{W}}$) ≤ 9. For the sake of notation simplicity, we will only consider one frame of the motion, and the i index will be dropped. However, results can be easily extended to a general case.

As every full-rank matrix can be expressed by an RQ decomposition, decomposing [$\mathbf{\Gamma}$, $\mathbf{\Omega}$, $\mathbf{\Lambda}$] should yield an identity matrix in the orthogonal factor in order to avoid ambiguities in the rotation. This implies that $\mathbf{\Gamma}$ must be an upper triangular matrix. In order to study the role of the quadratic deformation parameters, we applied different transformations to a synthetic cubic object. From the deformation observed, some instances of $\mathbf{M}_\mathrm{i}$ are not consistent with what is expected when modelling human body parts. For instance, deformation types that involve interpenetration of the shapes, or a twisting motion are not realistic. Based on these considerations, we defined the deformation matrices to be constrained as:

$$\Gamma = \begin{bmatrix} \Gamma_{11} & \Gamma_{12} & \Gamma_{13} \\ 0 & \Gamma_{22} & \Gamma_{21} \\ 0 & 0 & \Gamma_{33} \end{bmatrix}; \Omega = \begin{bmatrix} 0 & \Omega_{12} & \Omega_{13} \\ \Omega_{21} & 0 & \Omega_{23} \\ \Omega_{31} & \Omega_{32} & 0 \end{bmatrix}; \quad \Lambda = \begin{bmatrix} \Lambda_{11} & 0 & \Lambda_{13} \\ \Lambda_{21} & \Lambda_{22} & 0 \\ 0 & \Lambda_{32} & \Lambda_{33} \end{bmatrix}. \qquad (16)$$

The parameters for this model are estimated using a global non-linear optimization model generically termed bundle-adjustment. The

model is initialized with the results of the weighted factorization (for more details see [12]).

5 Experimental Results

We tested the weighted factorization algorithm with synthetic data, using noise as a simulation of deformations on a rigid body (for more details, see [12]). Qualitatively, we can see from Fig. 3 that the joint centres and joint axis resulting from the parameters of the weighted factorization method are consistent with the observed motion.

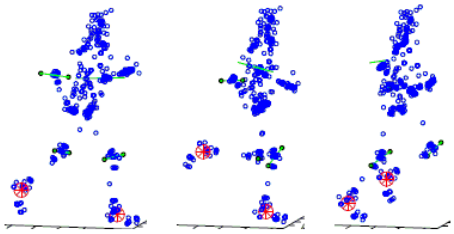

Fig. 3 Multiple joint parameter estimation, during a jogging motion. Knee and elbow articulations were modelled as hinge joints; the ankle joint was modelled as a universal joint.

Performance analysis on the reconstruction using the quadratic model showed improvements of 1 to 2 orders of magnitude (for more details, see [12]). Qualitatively, we can see in Fig. 4 the coherent reconstruction of the joint axis and joint centre.

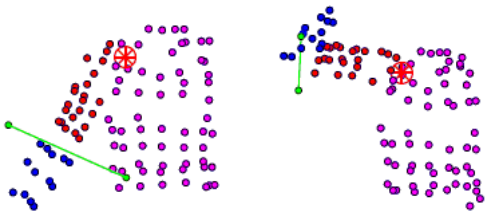

Fig. 4 Multiple joint parameter estimation on a flexing arm. The elbow is modelled as a hinge joint and the shoulder as a universal joint.

Conclusions

In this article we presented a method to automatically create 3D articulated human body models, assuming motion segmentation is known, based on 3D MOCAP systems. Our algorithms provide a more accurate rigid description of non-rigid bodies. Additionally, we presented a new quadratic model for non-rigid bodies, which can describe soft-tissue deformations.

Future research lines include incorporating automatic motion segmentation based on the motion capture data, a thoroughly validation of these models and a refined study of the quadratic model for non-rigid bodies in order to fully understand its applicability in this scenario.

ACKNOWLEDGMENTS

Partially supported by FCT, under ISR/IST plurianual funding (POSC program, FEDER), and grant MODI-PTDC/EEA-ACR/72201/2006.

References

[1] Baker, R.; "Gait analysis methods in rehabilitation", Journal of Neuro-Engineering and Rehabilitation, nº 1 , Vol. 3, pág. 1-4, 2006.

[2] Herda, L.; "Using Biomechanical Constraints to Improve Vídeo Based Motion Capture", PhD Thesis.

[3] Dariush, B.; "Human Motion Analysis for Biomechanics and Biomedicine", Machine Vision and Applications, nº 4, Vol. 14, pág. 202-205.

[4] Cappozzo, A.; Capello, A.; Crocce, U. D.; "Surface-marker Cluster Design Criteria for 3-D Bone Movement Reconstruction", IEEE Trans. on Biomedical Engineering, nº12, Vol. 44, pág. 1165-1174.

[5] Sati, M.; de Guise, J. A.; et al; "Quantitative Assessment of Skin-bone Movement at the Knee", The Knee, Vol. 3.

[6] Yan, J.; Pollefeys, M.; "A Factorization-based Approach for Articulated Motion Recovery", CVPR 2005, Vol. 2, pág. 1110 - 11115

[7] Tresadern, P.; Reid, I.; "Articulated Structure from Motion by Factorization", CVPR 2005, Vol. 2, pág. 815 - 821.

[8] Park, S. I.; Hodgins, J. K.; "Capturing and Animating Skin Deformation in Human Motion", SIGGRAPH 2006, pág. 881 - 889.

[9] Muller, M.; Heidelberger, B.; Teschner, M.; Gross, M. "Meshless Deformations Based on Shape Matching", ACM Trans. Graph. , nº3, Vol. 24, pág. 471 - 478.

[10] Kanade, T.; Morris D.; "Factorization Methods for Structure from Motion", Philosophical Trans.: Mathematical, Physical and Engineering Sciences, nº1740, Vol. 356, pág. 1153 - 1173.

[11] Irani, M. ; Anandan, P.; "Factorization with uncertainty", ECCV 2000, pág. 539—553.

[12] Fayad, J. K.; "Articulated 3D Human Modelling From Motion Capture Systems", MSc. Thesis.